This article was downloaded by: [Institute Of Atmospheric Physics]
On: 09 December 2014, At: 15:16
Publisher: Taylor & Francis
Informa Ltd Registered in England and Wales Registered Number: 1072954 Registered office: Mortimer House, 37-41 Mortimer Street, London W1T 3JH, UK

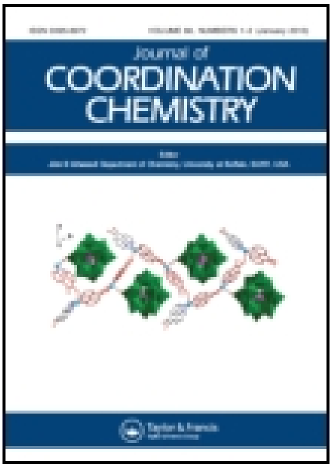

Journal of Coordination Chemistry
Publication details, including instructions for authors and subscription information:
http://www.tandfonline.com/loi/gcoo20

# Synthesis, structural characterization, and photocatalytic study of transition metal coordination polymers constructed from mixed ligands

Xiao-Guang Sang[a] & Xiao-Xia Liu[a]
[a] Department of Chemistry, Northeastern University, Shenyang, China

Accepted author version posted online: 04 Jul 2014.Published online: 24 Jul 2014.

Click for updates

To cite this article: Xiao-Guang Sang & Xiao-Xia Liu (2014) Synthesis, structural characterization, and photocatalytic study of transition metal coordination polymers constructed from mixed ligands, Journal of Coordination Chemistry, 67:13, 2301-2311, DOI: 10.1080/00958972.2014.939960

To link to this article: http://dx.doi.org/10.1080/00958972.2014.939960

PLEASE SCROLL DOWN FOR ARTICLE

Taylor & Francis makes every effort to ensure the accuracy of all the information (the “Content”) contained in the publications on our platform. However, Taylor & Francis, our agents, and our licensors make no representations or warranties whatsoever as to the accuracy, completeness, or suitability for any purpose of the Content. Any opinions and views expressed in this publication are the opinions and views of the authors, and are not the views of or endorsed by Taylor & Francis. The accuracy of the Content should not be relied upon and should be independently verified with primary sources of information. Taylor and Francis shall not be liable for any losses, actions, claims, proceedings, demands, costs, expenses, damages, and other liabilities whatsoever or howsoever caused arising directly or indirectly in connection with, in relation to or arising out of the use of the Content.

This article may be used for research, teaching, and private study purposes. Any substantial or systematic reproduction, redistribution, reselling, loan, sub-licensing, systematic supply, or distribution in any form to anyone is expressly forbidden. Terms &

*Journal of Coordination Chemistry*, 2014
Vol. 67, No. 13, 2301–2311, http://dx.doi.org/10.1080/00958972.2014.939960

Taylor & Francis
Taylor & Francis Group

# Synthesis, structural characterization, and photocatalytic study of transition metal coordination polymers constructed from mixed ligands

XIAO-GUANG SANG and XIAO-XIA LIU*

Department of Chemistry, Northeastern University, Shenyang, China

(*Received 28 December 2013; accepted 16 May 2014*)

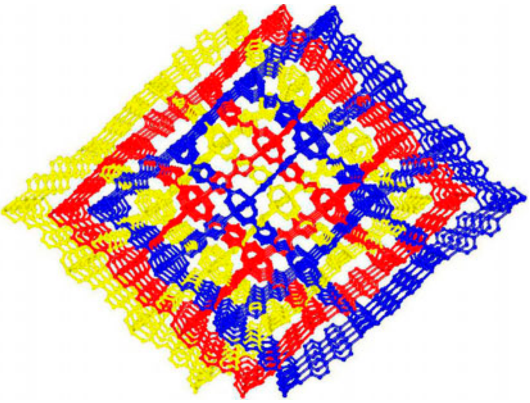

Three 3-D coordination polymers, $[Cu(cca)(4,4'\text{-bipy})]_n$ (**1**), $[Co_3(pda)_3(1,10'\text{-phen})_2]_n$ (**2**), and $[Co(pda)(1,10'\text{-phen})]_n$ (**3**), have been synthesized from 4-carboxycinnamic acid (cca), 1,4′-phenylenediacrylic acid (pda), 4,4′-bipyridine (4,4′-bipy), 1,10′-phenanthroline (1,10′-phen), and Cu and Co salts under different conditions. The X-ray crystal structures of these three complexes are presented. Complex **1** exhibits a threefold 3-D α-Po interpenetration network. Complex **2** with a 3-D framework with six-connected single α-Po framework constructed from $Co_3$ unit has been synthesized and characterized. Complex **3** shows a 3-D framework with bcu topology composed of 1-D rod-shaped secondary building units. Furthermore, the photocatalytic properties of **2** were studied. When excited by UV light, **2** exhibits photocatalytic activity, in 300 min, about 71% Rhodamine B decomposes.

*Keywords*: Coordination polymer; 3-D framework; Mixed ligands; Photocatalytic property

---

*Corresponding author. Email: xxliu@mail.neu.edu.cn

## 1. Introduction

The rational design and synthesis of coordination polymers has became a flourishing research area because of potential applications in magnetism, ion exchange, catalysis, gas separation, and electrical conductivity [1–7]. From the point of view of crystal engineering, the construction of coordination polymers with desired properties requires careful selection of the organic ligands [8–12]. Coordination polymers possessing various physical properties and diverse structural features arising from different types of ligands have been reported [13–19]. It is well known that carboxylate ligands play an important role in coordination chemistry and can adopt various coordination modes and link metal ions in different manners [20–22]. Among the large family of carboxylate ligands, 4-carboxycinnamic acid (cca) and 1,4′-phenylenediacrylic acid (pda) have attracted considerable interest [23, 24]. However, far less has been reported on this linker, which does not readily fit into a predictable template owing to flexibility and conformational freedom.

Recently, the introduction of secondary nitrogen-containing ligands into the metal-carboxylate system has been of interest not only because the use of mixed components can lead to novel structural features and interesting properties but also to make the construction process more controllable than with only a single ligand [25]. However, syntheses involving mixed ligands are more difficult due to the different solubility of mixed organic ligands and the competition between different organic ligands for the metal [26]. Numerous studies have shown that hydrothermal synthesis is a powerful method for the construction of coordination polymers from mixed ligands [27]. In such a relatively low temperature and autogenous pressure environment, the problem of different solubility for various ligands is minimized, and mixed ligands may be selected for efficient molecular building during the crystallization process.

Based on these considerations, we have prepared three new coordination polymers, $[Cu(cca)(4,4'\text{-bipy})]_n$ (**1**), $[Co_3(pda)_3(1,10'\text{-phen})_2]_n$ (**2**), and $[Co(pda)(1,10'\text{-phen})]_n$ (**3**). As promising photocatalysts, coordination polymers possess obvious merits for photocatalytic decomposition of organic dyes [28]. Up to now, the photocatalytic property of coordination polymers, however, has experienced limited research [29]. Here, the photocatalytic property of **2** is also studied.

## 2. Experimental

### 2.1. *Materials and general methods*

All purchased chemicals were of reagent grade and used without purification. Elemental analyses (C, H, and N) were performed on a Perkin-Elmer 2400 CHN elemental analyzer. FT/IR spectra were recorded from 4000 to 400 $cm^{-1}$ on an Alpha Centaur FTIR spectrophotometer using KBr pellets. TG analyses were performed on a Perkin-Elmer TGA7 instrument in flowing $N_2$ with a heating rate of 10 °C $min^{-1}$. The UV–visible adsorption spectrum was recorded using a Hitachi U-3010 UV–visible spectrometer. PXRD patterns were recorded on a Siemens D5005 diffractometer with Cu Kα ($\lambda = 1.5418$ Å) radiation.

### 2.2. *Preparation of 1*

Complex **1** was prepared from the mixture of $Cu(OAc)_2\cdot 4H_2O$ (0.030 g, 0.1 mM), $H_2cca$ (0.038 g, 0.2 mM), 4,4′-bipy (0.016 g, 0.1 mM), and 10 mL $H_2O$. The mixture was stirred and pH was adjusted to 5 with 1 M NaOH. After stirring for another 10 min, the mixture was transferred to a 23 mL Teflon-lined stainless steel bomb and kept at 180 °C under autogenous pressure for 5 days. The reaction system was cooled to room temperature during 24 h. A large amount of blue crystals of **1** were found. Yield: 81% (based on Cu). Anal. Calcd for $C_{15}H_{10}NO_4Cu$: C, 54.3%; H, 3.04%; N, 4.22%. Found: C, 53.91%; H, 3.12%; N, 4.15%.

### 2.3. *Preparation of 2*

Complex **2** was prepared from the mixture of $Co(OAc)_2{\cdot}4H_2O$ (0.050 g, 0.2 mM), $H_2$pda (0.044 g, 0.2 mM), 1,10′-phen (0.018 g, 0.1 mM), and 6 mL $H_2O$. The mixture was stirred and pH was adjusted to 5 with 1 M NaOH. After stirring for another 10 min, the mixture was transferred to a 23 mL Teflon-lined stainless steel bomb and kept at 120 °C under autogenous pressure for 4 days. The reaction system was cooled to room temperature during 24 h. A large amount of plate yellow crystals of **2** were obtained. Yield: 55% (based on Co). Anal. Calcd for $C_{60}H_{40}N_4O_{12}Co_3$: C, 60.77%; H, 3.40%; N, 4.72%. Found: C, 61.06%; H, 3.21%; N, 4.85%.

### 2.4. *Preparation of 3*

Complex **3** was prepared from the mixture of $Co(OAc)_2{\cdot}4H_2O$ (0.025 g, 0.1 mM), $H_2$pda (0.033 g, 0.15 mM), 1,10′-phen (0.027 g, 0.15 mM), and 10 mL $H_2O$. The mixture was stirred and pH was adjusted to 6 with 1 M NaOH. After stirring for another 10 min, the mixture was transferred to a 23 mL Teflon-lined stainless steel bomb and kept at 150 °C under autogenous pressure for 3 days. The reaction system was cooled to room temperature during 24 h. A large amount of brown crystals of **3** were found. Yield: 67% (based on Co). Anal. Calcd for $C_{24}H_{16}N_2O_4Co$: C, 63.31%; H, 3.54%; N, 6.15%. Found: C, 63.12%; H, 3.39%; N, 6.31%. IR ($cm^{-1}$): 1561 (s), 1389 (s), 1101(s), 976 (s), 852 (s), 726 (s).

### 2.5. *Photocatalytic experiment*

The photocatalytic activities of the samples were evaluated by the degradation of Rhodamine B (RhB) in the aqueous solution. Seventy milliliters RhB aqueous solution with concentration of $10^{-5}$ M was mixed with 30 mg catalysts, which was exposed to illumination. Before turning on the lamp, the suspension containing RhB and photocatalyst was magnetically stirred in a dark condition for 40 min till an adsorption–desorption equilibrium was established. Samples were then taken out regularly from the reactor and centrifuged immediately for separation of any suspended solid. The transparent solution was analyzed by a UV–vis spectrometer. An 11 W germicidal lamp ($\lambda = 254$ nm) served as a UV light source. Langmuir–Hinshelwood (L–H) equation ($r_0 = k_0C_0/1 + K_0C_0$) is employed to quantify the degradation reaction of RhB ($r_0$ represents the initial rate, $k_0$ represents the kinetic rate constant, and $K_0$ represents the adsorption coefficient of the reactant RhB). As the value of $C_0$ is small, $K_0C_0 \ll 1$, the L–H rate expression can simply be the first-order rate expression: $r_0 = dC_0/dt = k_0C_0$. This equation can be solved to obtain ln $(C/C_0) = -k_0t$. Based on Lambert–Beer law, $C/C_0 = I/I_0$, the equation can reduce to ln $(I/I_0) = -k_0t$ finally.

### 2.6. *X-ray crystallography*

Suitable single crystals of **1**–**3** were carefully selected under an optical microscope and glued on glass fibers. Structural measurements were performed on a Bruker AXS SMART APEX II CCD diffractometer at 298 K. The structures were solved by the direct method and refined by full-matrix least-squares on $F^2$ using the SHELXTL 97 crystallographic software package, and anisotropic thermal parameters were used to refine all non-hydrogen atoms [30, 31]. Carbon-bound hydrogen atoms were placed in geometrically calculated positions. Oxygen-bound hydrogen atoms were located in the difference Fourier maps, kept in that position, and refined with isotropic temperature factors. Further details of the X-ray structural analysis are given in table 1. Selected bond lengths and angles are listed in tables 2 and 3. Further details of the crystal structure determination have been deposited to the Cambridge Crystallographic Data Center as supplementary publication. CCDC 975491, 905276, and 905277 for **1**–**3** contain the supplementary crystallographic data for this article.

## 3. Results and discussion

### 3.1. *Structure description*

For **1**, there exists one crystallographically independent Cu atom in its fundamental unit, which adopts square-pyramidal geometry. Cu1 connects with four oxygens and one nitrogen from cca and 4,4′-bipy ligands, respectively [figure 1(a)]. Such two Cu atoms are connected by four carboxylates with Cu···Cu distance of 2.986 Å. The axis sites of each $Cu_2$ unit are occupied by two 4,4′-bipy ligands. Such arrangement of the carboxylate oxygens and nitrogens results in an octahedral $[Cu_2(CO_2)_4N_2]$ secondary building units (SBUs). Each SBU links with six others through four cca liangds, two 4,4′-bipy, and generates an extended neutral 3-D network. The overall topology of the 3-D framework can be described as the

Table 1. Crystal data and structure refinements for **1**–**3**.

| | **1** | **2** | **3** |
|---|---|---|---|
| Empirical formula | $C_{15}NO_4H_{10}Cu$ | $C_{60}H_{40}N_4O_{12}Co_3$ | $C_{24}H_{16}N_2O_4Co$ |
| Formula weight | 331.78 | 1185.75 | 455.32 |
| Crystal system | Monoclinic | Triclinic | Monoclinic |
| Space group | *C2/c* | *P-1* | *C2/c* |
| $a$ (Å) | 16.773(5) | 8.1471(8) | 25.645(8) |
| $b$ (Å) | 20.409(6) | 13.6900(14) | 11.555(4) |
| $c$ (Å) | 10.371(3) | 13.8330(14) | 7.012(2) |
| $\alpha$ (°) | 90 | 62.541(2) | 90 |
| $\beta$ (°) | 115.502(4) | 86.678(2) | 99.982(4) |
| $\gamma$ (°) | 90 | 87.729(2) | 90 |
| $V$ (Å$^3$) | 3204.4(16) | 1366.6(2) | 2046.3(11) |
| $Z$ | 8 | 1 | 4 |
| $D_{calcd}$/(g cm$^{-3}$) | 1.375 | 1.441 | 1.478 |
| $F$ (0 0 0) | 1344 | 605 | 932 |
| Reflections collected | 9804 | 6917 | 5908 |
| Reflections unique | 2781 | 4739 | 1810 |
| $R$(int) | 0.0212 | 0.0135 | 0.0190 |
| Goodness-of-fit on $F^2$ | 1.056 | 1.112 | 1.413 |
| $R_1[I > 2\sigma(I)]$ | 0.0502 | 0.0505 | 0.0522 |
| $wR_2$ $[I > 2\sigma(I)]$ | 0.1654 | 0.1568 | 0.2136 |

Notes: $R_1 = \Sigma||F_o| - |F_c||/\Sigma|F_o|$; $wR_2 = \Sigma[w(F_o^2 - F_c^2)^2]/\Sigma[w(F_o^2)^2]^{1/2}$.

Table 2. Selected bond lengths for **1–3**.

| | | | |
|---|---|---|---|
| **1** | | | |
| Cu(1)–O(1)#3 | 2.078(3) | Cu(1)–O(2) | 2.037(3) |
| Cu(1)–O(3)#1 | 2.029(3) | Cu(1)–O(4)#2 | 2.049(3) |
| Cu(1)–N(1) | 2.056(4) | | |
| **2** | | | |
| Co(1)–O(2) | 2.148(2) | Co(1)–O(2)#1 | 2.148(2) |
| Co(1)–O(3) | 2.188(2) | Co(1)–O(3)#1 | 2.188(2) |
| Co(1)–O(6) | 2.165(2) | Co(1)–O(6)#1 | 2.165(2) |
| Co(2)–O(5) | 2.070(2) | Co(2)–O(3) | 2.099(2) |
| Co(2)–O(1) | 2.086(2) | Co(2)–N(1) | 2.241(2) |
| Co(2)–N(2) | 2.237(3) | | |
| **3** | | | |
| Co(1)–O(1)#2 | 2.162(2) | Co(1)–O(1)#3 | 2.162(2) |
| Co(1)–O(2) | 2.115(2) | Co(1)–O(2)#1 | 2.115(2) |
| Co(1)–N(1) | 2.332(2) | Co(1)–N(1)#1 | 2.332(2) |

Notes: Symmetry transformations used to generate equivalent atoms for **1**: #1: $x-1/2$, $y-1/2$, $z$; #2: $-x+3/2$, $y-1/2$, $-z+5/2$; #3: $-x+1$, $y$, $-z+5/2$; for **2**: #1: $-x-2$, $-y$, $-z+1$; for **3**: #1: $-x+1$, $y$, $-z+3/2$; #2: $-x+1$, $-y$, $-z+1$; #3: $x$, $-y$, $z+1/2$.

Table 3. Selected angles for **1**–**3**.

| | | | |
|---|---|---|---|
| **1** | | | |
| O(2)–Cu(1)–O(1)#3 | 86.04(13) | O(2)–Cu(1)–O(4)#2 | 90.05(15) |
| O(3)#1–Cu(1)–O(2) | 165.46(13) | O(3)#1–Cu(1)–O(4)#2 | 89.07(15) |
| O(3)#1–Cu(1)–O(1)#3 | 88.03(15) | O(4)#2–Cu(1)–O(1)#3 | 152.35(13) |
| O(2)–Cu(1)–N(1) | 97.83(12) | O(3)#1–Cu(1)–N(1) | 96.64(13) |
| O(4)#2–Cu(1)–N(1) | 98.92(13) | N(1)–Cu(1)–O(1)#3 | 108.73(13) |
| **2** | | | |
| O(2)#1–Co(1)–O(2) | 180.0 | O(2)#1–Co(1)–O(6)#1 | 90.71(9) |
| O(2)–Co(1)–O(6)#1 | 89.29(9) | O(2)#1–Co(1)–O(6) | 89.29(9) |
| O(2)–Co(1)–O(6) | 90.71(9) | O(6)–Co(1)–O(3)#1 | 89.23(8) |
| O(6)#1–Co(1)–O(6) | 180.00(19) | O(2)#1–Co(1)–O(3) | 93.20(8) |
| O(2)#1–Co(1)–O(3)#1 | 86.80(8) | O(2)–Co(1)–O(3) | 86.80(8) |
| O(2)–Co(1)–O(3)#1 | 93.20(8) | O(6)#1–Co(1)–O(3) | 89.23(8) |
| O(6)#1–Co(1)–O(3)#1 | 90.77(8) | O(6)–Co(1)–O(3) | 90.77(8) |
| O(3)#1–Co(1)–O(3) | 180.00(10) | O(5)–Co(2)–O(1) | 94.24(11) |
| O(5)–Co(2)–N(1) | 153.45(10) | O(5)–Co(2)–O(3) | 100.52(9) |
| O(1)–Co(2)–N(1) | 89.19(9) | O(1)–Co(2)–O(3) | 102.51(9) |
| O(3)–Co(2)–N(1) | 104.42(9) | O(5)–Co(2)–N(2) | 84.74(10) |
| N(2)–Co(2)–N(1) | 73.34(10) | O(1)–Co(2)–N(2) | 130.95(10) |
| O(3)–Co(2)–N(2) | 125.97(10) | | |
| **3** | | | |
| O(2)–Co(1)–O(2)#1 | 116.71(12) | O(2)–Co(1)–O(1)#2 | 96.03(8) |
| O(2)–Co(1)–O(1)#2 | 96.03(8) | O(2)#1–Co(1)–O(1)#2 | 86.33(8) |
| O(2)#1–Co(1)–O(1)#2 | 86.33(8) | O(2)–Co(1)–O(1)#3 | 86.33(8) |
| O(2)–Co(1)–O(1)#3 | 86.33(8) | O(2)#1–Co(1)–O(1)#3 | 96.03(8) |
| O(1)#2–Co(1)–O(1)#3 | 175.53(9) | O(2)–Co(1)–N(1)#1 | 157.07(9) |
| O(2)#1–Co(1)–N(1)#1 | 86.20(8) | O(1)#2–Co(1)–N(1) | 90.46(8) |
| O(1)#2–Co(1)–N(1)#1 | 85.90(8) | O(1)#3–Co(1)–N(1) | 85.90(8) |
| O(1)#3–Co(1)–N(1)#1 | 90.46(8) | N(1)#1–Co(1)–N(1) | 70.92(13) |
| O(2)–Co(1)–N(1) | 86.20(8) | O(2)#1–Co(1)–N(1) | 157.07(9) |

Notes: Symmetry transformations used to generate equivalent atoms for **1**: #1: $x-1/2$, $y-1/2$, $z$; #2: $-x+3/2$, $y-1/2$, $-z+5/2$; #3: $-x+1$, $y$, $-z+5/2$; for **2**: #1: $-x-2$, $-y$, $-z+1$; for **3**: #1: $-x+1$, $y$, $-z+3/2$; #2: $-x+1$, $-y$, $-z+1$; #3: $x$, $-y$, $z+1/2$.

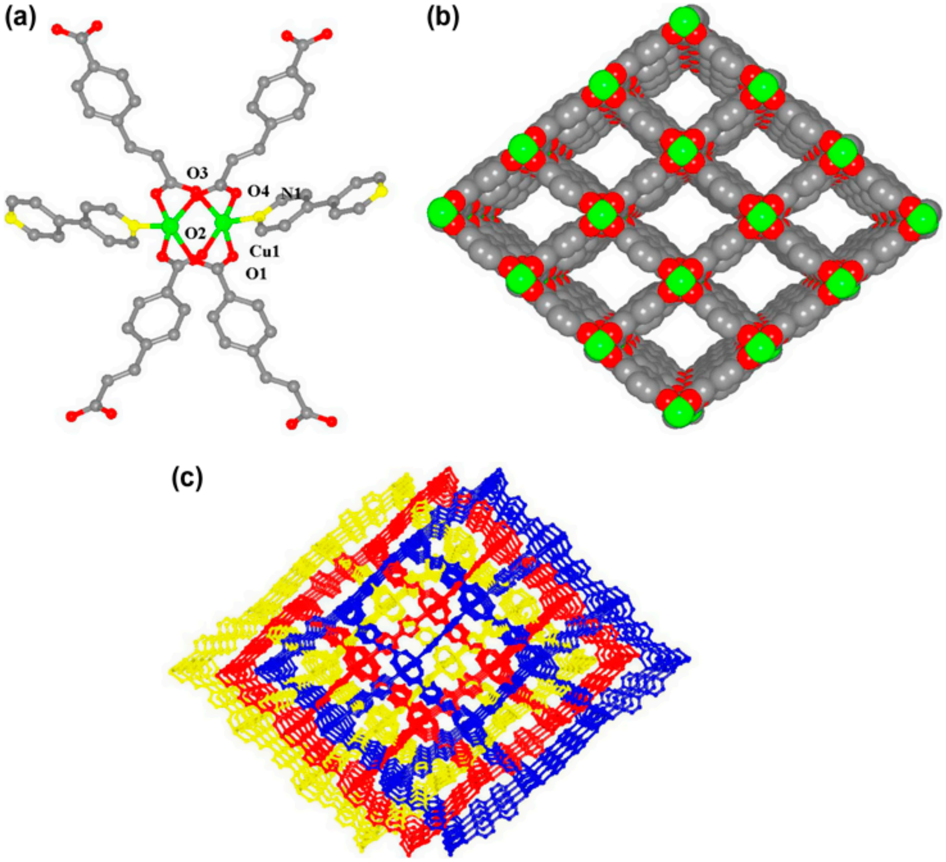

Figure 1. (a) The fundamental unit of **1** showing the coordination geometry of $Zn^{2+}$ ions (hydrogens are omitted for clarity); (b) the 3-D framework of **1**; (c) scheme representation of threefold interpenetration network of **1**.

$\alpha$-Po net, which possesses large cavities [figure 1(b)]. These large voids formed in one single 3-D network allow incorporation of other two identical networks, thus giving a threefold interpenetrated $\alpha$-Po network [figure 1(c)].

Single-crystal X-ray analysis shows that the structure of **2** contains $Co_3$ unit. There exist two crystallographically independent Co atoms in the fundamental unit, which exhibit two kinds of coordination geometries. Co1 lies at the center of symmetry and connects with six oxygens from six pda ligands (bond distances range from 2.148 to 2.188 Å and bond angles are in the range from 86.80° to 180.0°). This leads to an octahedral geometry of Co1. On the contrary, Co(2) exists in a highly distorted trigonal bipyramidal geometry, being ligated by two nitrogens with Co–N bond distances 2.237 and 2.241 Å from a chelating 1,10′-phen ligand, three oxygens from three pda ligands with bond distances in the range from 2.070 to 2.099 Å [figure 2(a)]. Moreover, the pda ligands adopt two kinds of coordination modes; in the first type, the pda ligand contains two bridging carboxylate groups while in the second pad ligand, one carboxylate adopts monodentate bridging coordination mode; the other adopt chelating–bridging coordination mode. As such, each trinuclear metal cluster is surrounded by eight organic ligands with six bridging pda and two chelating 1,10′-phen.

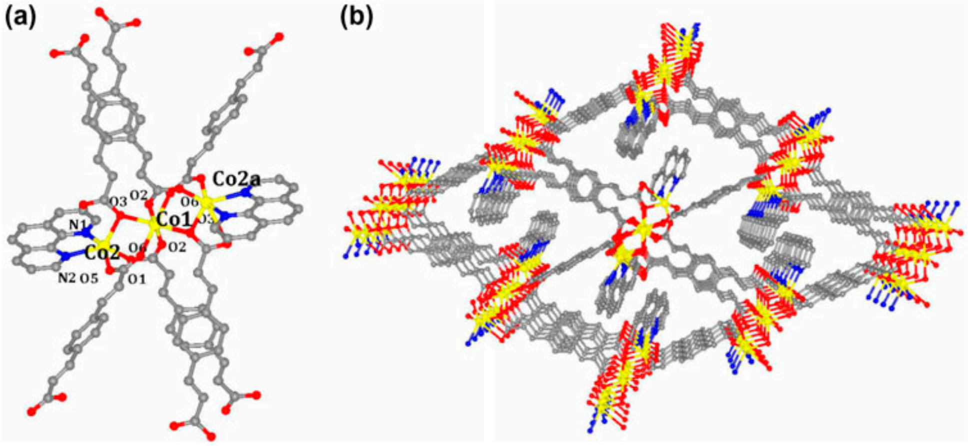

Figure 2. (a) The fundamental unit of **2** showing the coordination geometry of $Co^{2+}$ ions (hydrogens are omitted for clarity). (b) The 3-D framework of **2**.

The cluster, therefore, defines a six-connected node. Each trinuclear Co core is further linked to six nearest neighbors through six pda ligands, thus leading to a 3-D framework [figure 2(b)].

Single-crystal X-ray diffraction analysis reveals that there exists only one crystallographically independent Co atom in the fundamental unit; Co1 connects with four oxygens from four pda ligands (Co–O distances and O–Co–O bond angles range from 2.115 to 2.162 Å and 86.33° to 175.53°). The other two coordination sites are occupied by nitrogens from one 1,10′-phen. This results in a slightly distorted octahedron coordination mode of **3** [figure 3(a)]. Two carboxylate groups of pda ligand both adopt bridging connection mode and link the adjacent Co atoms together. This results in a 1-D Co–C–O chain, which can be seen as 1-D rod-shaped SBUs [figure 3(b)]. One rod-shaped SBU connects with four neighboring rod-shaped SBUs with pda ligands and results in the 3-D structure of **3** [figure 3(c)]. Up to now, many MOFs have been constructed from 1-D rod-shaped SBUs and from Yaghi's theory the network can be defined as bcu topology [figure 3(d)]. To our knowledge, some coordination polymers constructed from pda have been synthesized, but coordination polymers that possess similar structural features with **2** and **3** have not been reported [32–34].

Although **2** and **3** were synthesized under hydrothermal conditions, but pH and temperature of these two reaction systems are different, which leads to different connection modes of pda ligands and results in the structural differences between **2** and **3**. To our knowledge, this phenomenon has been reported by other researchers [35, 36].

### 3.2. *Photocatalytic property study*

Photocatalytic activity property studies were investigated by the degradation of RhB. When excited by UV light, **2** exhibits photocatalytic activity, in 300 min, about 71% RhB decompose and the rate constant is 0.00514 $min^{-1}$ [figures 4(a) and (b)]. We also studied the degradation of RhB under the irradiation of UV light without **2** and found only about 3% RhB

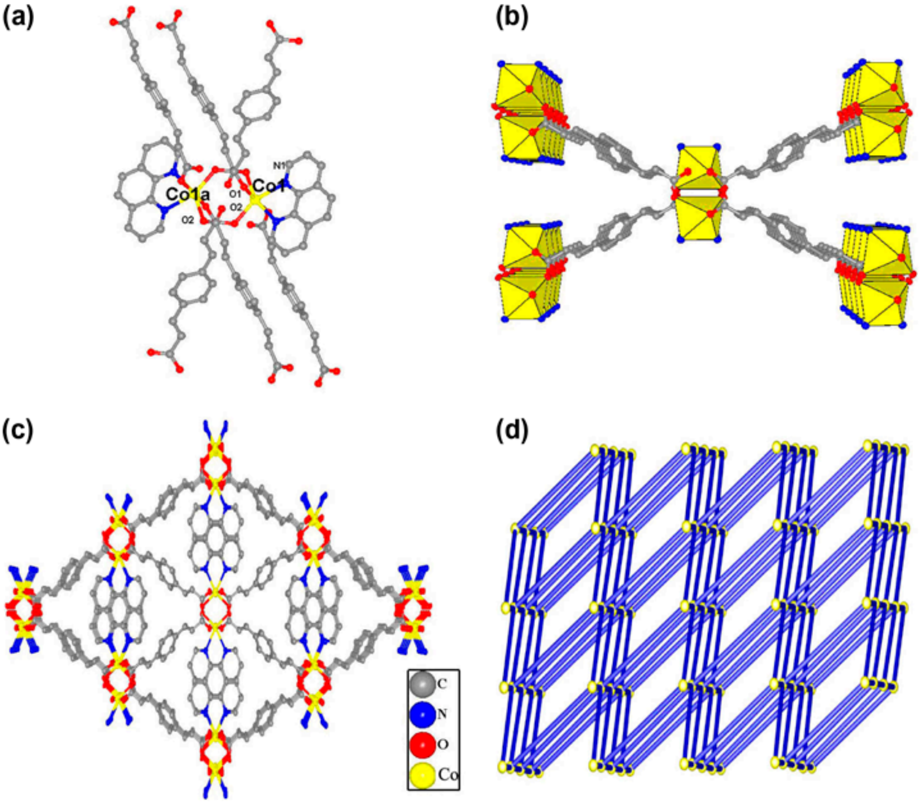

Figure 3. (a) The fundamental unit of **3** showing the coordination geometry of $Co^{2+}$ ions (hydrogens are omitted for clarity); (b) 1-D rod-shaped SBUs of **3**; (c) the 3-D framework of **3**. (d) The scheme representation of the bcu topology of **3**.

were decomposed (figure S1, see online supplemental material at http://dx.doi.org/10.1080/00958972.2014.939960). Based on this point, we can attribute the decomposition of RhB to the photocatalytic property of **2**. For photocatalytic degradation reaction, the activity of recycled catalyst is a very important factor to determine the performance of a photocatalyst. Here, the photocatalytic reaction is re-examined five times (figure 5). The recycled complex **2** still exhibits excellent catalytic property and the relationship of degradation rate and time is very similar between every cycle, which indicates its high stability during the decomposition process of organic dyes.

### 3.3. *Photocatalytic mechanism study*

It is important to study the decomposition mechanism of RhB under different photocatalysts and conditions. Based on the experimental findings and observations, we speculate the mechanism as follows (scheme 1). For **2**, under the irradiation of UV light, the electrons are excited from the valence band (VB) and transferred to the conduction band, simultaneously, positive charged holes are be formed in VB [scheme 1(a)]. After migrating to the surface of **2**, the electrons reduce the oxygen ($O_2$) to superoxide radical ($O_2^{-}$) and holes oxidize the hydroxyl ($H_2O$) to hydroxyl radicals (·OH). These oxygen radicals and hydroxyl radicals are responsible for the degradation of RhB.

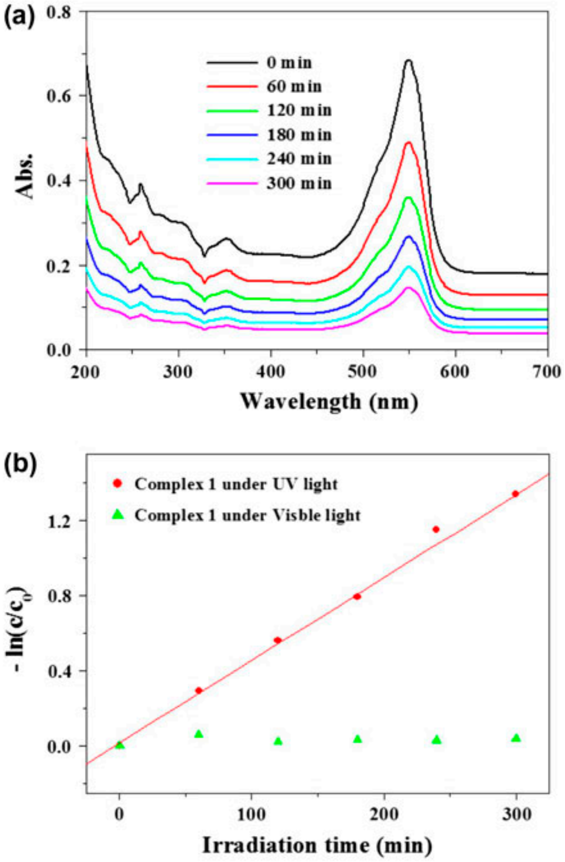

Figure 4. (a) UV–vis absorption spectra of RhB solution degraded by **2** under UV light; (b) curve of degradation rate for RhB by **2** under different conditions as the function of irradiation time.

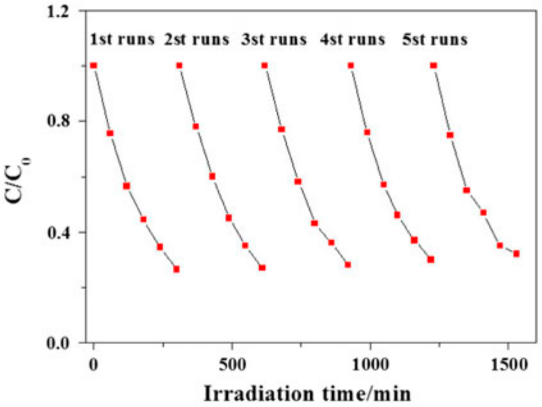

Figure 5. Cycling runs of the photocatalytic degradation of RhB in the presence of **2**.

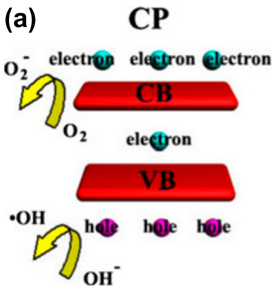

$\text{Coordination polymer} + h\gamma \rightarrow h^+ + e^-$
$h^+ + OH^- \rightarrow \cdot OH$
$h^+ + H_2O \rightarrow OH + H^+$
$e^- + O_2 \rightarrow O_2^-$
$O_2^- + H^+ \rightarrow HO_2\cdot$
$2HO_2\cdot \rightarrow O_2 + H_2O_2$
$H_2O_2 + \cdot O_2^- \rightarrow OH + OH^- + O_2$
$RhB + OH \rightarrow CO_2 + H_2O$

Scheme 1. Diagram of the photocatalytic mechanism for coordination polymer under UV light.

## 4. Conclusion

We have synthesized three new coordination polymers. Complex **1** shows a threefold interpenetration α-Po network. Complex **2** is constructed from a $Co_3$ unit and exhibits a 3-D framework. Complex **3** also exhibits a 3-D framework composed of 1-D rod-shaped secondary building units. Although **2** and **3** were synthesized with the same materials, different connection modes of pda ligands results in the structural differences between them. The photocatalytic properties of **2** were studied.

## Funding

This work was supported by Research Foundation for Doctoral Program of Higher Education of China [grant number 20120042110024].

## References

[1] D.R. Turner, J. Strachan-Hatton, S.R. Batten. *CrystEngComm.*, **10**, 34 (2007).
[2] J.W. Cheng, J. Zhang, S.T. Zheng, G.Y. Yang. *Chem. Eur. J.*, **14**, 88 (2008).
[3] Y. Yang, M.H. Zeng, L.J. Zhang, H. Liang. *J. Coord. Chem.*, **62**, 886 (2009).
[4] Y.E. Cheon, M.P. Suh. *Chem. Commun.*, 2296 (2009).
[5] P.P. Long, Q. Zhao, J.X. Dong, J.P. Li. *J. Coord. Chem.*, **62**, 1959 (2009).
[6] X.X. Xu, X. Zhang, X.X. Liu, T. Sun, E.B. Wang. *Cryst. Growth Des.*, **10**, 2272 (2010).
[7] L.L. Wen, D.E. Wang, Y.J. Chen, X.G. Meng, D.F. Li, S.M. Lan. *J. Coord. Chem.*, **62**, 789 (2009).
[8] B. Zhao, X.Y. Chen, Z. Chen, W. Shi, P. Cheng, S.P. Yan, D.Z. Liao. *Chem. Commun.*, 3113 (2009).
[9] Z.R. Ranjbar, S. Hamidi, F. Heshmatpour, A. Morsali. *J. Coord. Chem.*, **62**, 2022 (2009).
[10] A.A. Rexit. *J. Coord. Chem.*, **62**, 1373 (2009).
[11] D.E. Wang, Z.F. Tian, F. Wang, L.L. Wen, D.F. Li. *J. Inorg. Organomet. Polym.*, **19**, 196 (2009).
[12] X.L. Wang, Y.F. Bi, G.C. Liu, H.Y. Lin, T.L. Hu, X.H. Bu. *CrystEngComm.*, **10**, 349 (2009).
[13] G.X. Liu, J. Yan, L.F. Huang, X.M. Ren. *J. Inorg. Organomet. Polym.*, **19**, 243 (2009).
[14] H.Y. Lin, X.L. Wang, H.L. Hu, B.K. Chen, G.C. Liu. *Solid State Sci.*, **11**, 643 (2009).
[15] X.L. Wang, B.K. Chen, H.Y. Lin, H.L. Hu, J. Li. *Transition Met. Chem.*, **34**, 307 (2009).
[16] M. Müller, X.N. Zhang, Y.M. Wang, R.A. Fischer. *Chem. Commun.*, 119 (2009).
[17] C.L. Ma, Q.L. Li, R.F. Zhang. *J. Inorg. Organomet. Polym.*, **19**, 208 (2009).
[18] S.Z. Zhan, M. Li, J.Z. Hou, J. Ni, D. Li, X.C. Huang. *Chem. Eur. J.*, **14**, 8916 (2008).
[19] Q.X. Yao, W.M. Xuan, H. Zhang, C.Y. Tua, J. Zhang. *Chem. Commun.*, 1840 (2009).
[20] R.L. Sang, L. Xu. *Chem. Commun.*, 6143 (2009).
[21] Y.G. Huang, X.T. Wang, F.L. Jiang, S. Gao, M.Y. Wu, Q. Gao, W. Wei, M.C. Hong. *Chem. Eur. J.*, **14**, 10340 (2008).

[22] X.L. Wang, B.K. Chen, G.C. Liu, H.Y. Lin, H.L. Hu, Y.Q. Chen. *J. Inorg. Organomet. Polym.*, **19**, 176 (2009).
[23] X.X. Xu, X. Zhang, X.X. Liu, L.S. Wang, E.B. Wang. *CrystEngComm.*, **14**, 3264 (2012).
[24] K.L. Huang, X. Liu, J.K. Li, Y.W. Ding, X. Chen, M.X. Zhang, X.B. Xu, X.J. Song. *Cryst. Growth Des.*, **10**, 1508 (2010).
[25] X.X. Xu, Y. Ma, E. Wang. *J. Solid State Chem.*, **180**, 3136 (2007).
[26] X.L. Wang, C. Qin, Y.Q. Lan, K.Z. Shao, Z.M. Su, E.B. Wang. *Chem. Commun.*, 410 (2009).
[27] X.X. Xu, Y. Lu, E.B. Wang, Y. Ma, X.L. Bai. *Inorg. Chim. Acta*, **358**, 4575 (2005).
[28] M.C. Das, H. Xu, Z.Y. Wang, G. Srinivas, W. Zhou, Y.F. Yue, V.N. Nesterov, G.D. Qian, B.L. Chen. *Chem. Commun.*, **47**, 11715 (2011).
[29] C. Wang, Z.G. Xie, K.E. DeKrafft, W.B. Lin. *J. Am. Chem. Soc.*, **133**, 13445 (2011).
[30] G.M. Sheldrick. *SHLEXL97, Program for Crystal Structure Refinement*, University of Göttingen, Germany (1997).
[31] G.M. Sheldrick. *SHLEXL97, Program for Crystal Structure Solution*, University of Göttingen, Germany (1997).
[32] K.J. Wei, Y.S. Xie, J. Ni, M. Zhang, Q.L. Liu. *Cryst. Growth Des.*, **6**, 1341 (2006).
[33] Q.R. Fang, G.S. Zhu, M. Xue, Q.L. Zhang, J.Y. Sun, X.D. Guo, S.L. Qiu, S.T. Xu, P. Wang, D.J. Wang, Y. Wei. *Chem. Eur. J.*, **12**, 3754 (2006).
[34] M.L. Zhang, J.J. Wang, Y.X. Ren Lei IV. *J. Coord. Chem.*, **64**, 3585 (2011).
[35] F.L. Hu, X. Yang, Y.J. Li. *J. Coord. Chem.*, **65**, 4245 (2012).
[36] M.L. Liu, Y.X. Wang, W. Shi, J.Z. Cui. *J. Coord. Chem.*, **65**, 1915 (2012).